Journal of Alloys and Compounds 489 (2010) L9–L12

Contents lists available at ScienceDirect

Journal of Alloys and Compounds

journal homepage: www.elsevier.com/locate/jallcom

Letter

Morphologies of $GdBO_3$:Eu^{3+} one-dimensional nanomaterials

Zhi Yang[a,*], Ya-lin Wen[a], Nan Sun[a], Yu-fei Wang[a], Yan Huang[b], Zhen-hua Gao[b], Ye Tao[b]

[a] Faculty of Chemistry and Chemical Engineering, Yunnan Normal University, Kunming 650092, Yunnan Province, PR China
[b] Beijing Synchrotron Radiation Facilities, Institute of High Energy Physics, Chinese Academy of Sciences, Beijing 100049, PR China

ARTICLE INFO

Article history:
Received 26 April 2009
Received in revised form
15 September 2009
Accepted 16 September 2009
Available online 23 September 2009

Keywords:
Nanostructured materials
Rare earth alloys and compounds
AAO template
Liquid–solid reactions
Luminescence

ABSTRACT

Europium doped gadolinium orthoborate nanorods and nanoribbons were morphology-controlled grown on the porous anodic aluminum oxide (AAO) template surface via a hydrothermal process combined with high-temperature calcination. The morphologies, crystal structures and luminescent properties of the as-prepared nanomaterials were characterized by scanning electron microscopy (SEM), X-ray diffraction (XRD) and photoluminescence (PL) spectra. The morphologies of the nanomaterials were controlled by the calcination temperature. If calcined at 1000 °C, the morphology of the $GdBO_3$:Eu^{3+} one-dimensional materials is nanorods; when calcined at 800 and 600 °C, the shapes of the Eu-doped $GdBO_3$ are nanoribbons. If treated at 900 °C, the as-prepared samples are composed of nanorods and nanoribbons.

The changed morphologies of the as-prepared nanomaterials obtained from different calcination temperatures were explained according to the structural phase transition of $GdBO_3$. The PL spectrum shows that the characteristic emission of $GdBO_3$:Eu^{3+} one-dimensional nanomaterials is the $^5D_0 \rightarrow {}^7F_1$ transition.

1. Introduction

Due to their high vacuum ultraviolet (VUV) transparency, good VUV absorption and exceptional optical damage threshold in the VUV range, rare earth orthoborates ($REBO_3$, RE = Gd and Y) with the hexagonal vaterite-type structure are an interesting class of materials [1–3]. $REBO_3$:Eu^{3+} is one of the best red phosphors, and widely applied in plasma display panels (PDP) and Hg-free lamps. As the local symmetry of the rare earth ions is centrosymmetric in $REBO_3$ structure, so the characteristic emission of $REBO_3$:Eu^{3+} powders prepared by the common solid state reaction is $^5D_0$–$^7F_1$ typical magnetic dipole transition, and $^5D_0$–$^7F_2$ typical electric dipole transition is weak [3–5], which give rise to an orange–red emission instead of a red one, hence, it is not ideal for its application in display and lamp applications.

Recently, some new methods, such as sol–gel method [6,7], spray pyrolysis [8], combustion synthesis [9], hydrothermal/solvothermal synthesis [10–23], co-precipitation method [24], electrospinning method [25], etc., have been employed to reduce the reaction temperature for obtaining $REBO_3$:Eu^{3+} nanomaterials. $REBO_3$:Eu^{3+} nanoparticles [10], nanotube and nanowires [25], drum-like microcrystals [13], donut-like assemblies [11,19], etc., have been successfully synthesized. The luminescent properties of the $REBO_3$:Eu^{3+} nanomaterials have been obviously improved. Some research groups [24–27] reported that the nanosized YBO_3:Eu^{3+} is just the desirable VUV phosphor, which realized the improvements in both fluorescent intensity and chromaticity in comparison with bulk YBO_3:Eu^{3+}.

The synthesis methods, morphology and luminescence of the nanosized $REBO_3$:Eu^{3+} were widely studied [6–27]. Especially, the hydrothermal/solvothermal method is widely used to synthesize rare earth orthoborates powders as well as to control their microstructures [10–23]. The controlled synthesis of nanomaterials with uniform size and morphology has attracted much attention due to their novel properties for theoretical studies and potential applications in optics, electronics, magnetism and catalysis [28–30]. There have been many reports on the preparation of various nanomaterials since last decades [31–34]. AAO template has a highly ordered nanoporous array with adjustable and controllable pore diameter, and has been widely used to prepare one-dimensional materials and thin films [35–37]. Unfortunately, up to now, there are few reports on the preparation of $REBO_3$:Eu^{3+} thin films and one-dimensional materials on the AAO template surface by a hydrothermal process [38]. In this paper, the preparation of $GdBO_3$:Eu^{3+} one-dimensional materials on the porous AAO template surface by a hydrothermal method combined with high-temperature calcination was first reported, the morphologies and luminescent properties of the nanomaterials were investigated.

2. Experimental

For the preparation of $Gd_{0.95}Eu_{0.05}BO_3$/AAO products, stoichiometric amounts of Gd_2O_3 and Eu_2O_3 were dissolved in 50 ml distilled water acidified by the addition

* Corresponding author. Tel.: +86 871 5516063; fax: +86 871 5516061.
E-mail address: kmyangz@hotmail.com (Z. Yang).

0925-8388/$ – see front matter © 2009 Elsevier B.V. All rights reserved.
doi:10.1016/j.jallcom.2009.09.073

of nitric acid. After the complete dissolution of these oxides, the amount of boric acid (80 mol% excess) was first added into the solution, then a dilute $NH_3 \cdot H_2O$ (1:1) solution was added dropwise until the pH value of the solution reached 8. Finally, the total volume of the solution is 80 ml, and the amount of all rare earth ions is 0.02 mol/l. The final solution and AAO template were transferred into a Teflon-lined stainless steel autoclave with a volume of 100 ml. After the autoclave was sealed tightly, placed in a temperature-controlled electric oven, heated at 240 °C for 12 h and then cooled down to room temperature in the furnace. The $Gd_{0.95}Eu_{0.05}BO_3$/AAO products were collected from the solution, washed with distilled water and ethanol for several times. Finally the $Gd_{0.95}Eu_{0.05}BO_3$/AAO products were dried at 80 °C for 5 h, and then calcined at 600, 800, 900 and 1000 °C for 10 h, respectively.

The purity of Gd_2O_3 and Eu_2O_3 is 99.99%. Boric acid and other chemicals are all analytical pure (A.R.). Porous AAO template was provided by Whatman (Anodisc 25, 200 nm). X-ray diffraction (XRD) studies were carried out on a Rigaku D/max-38 X-ray powder diffractometer using Cu Kα radiation. The morphologies of the as-prepared products were characterized by XL 30ESEM-TMP scanning electron microscopy. The VUV data were collected through remote access on 4B8 VUV spectroscopy station at the Beijing Synchrotron Radiation Facilities (BSRF) under a dedicated synchrotron mode (2.5 GeV, 250–150 mA) at room temperature.

3. Results and discussion

3.1. Phase formation

Fig. 1 shows the XRD pattern of the hydrothermally synthesized $GdBO_3$:Eu^{3+}/AAO products (at 240 °C for 12 h). All diffraction peaks in Fig. 1 could be readily indexed according to the hexagonal phase of $GdBO_3$, as listed in JCPDS files (No. 74-1932), its lattice constants were calculated to be $a = b = 3.8366(9)$ Å, $c = 8.917(2)$ Å. No additional diffraction peaks of other phases have been found, indicating that all Eu^{3+} ions have been effectively doped into the host lattice.

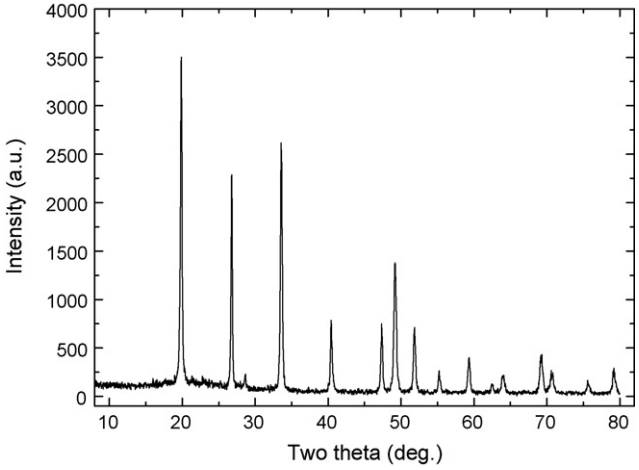

Fig. 1. XRD pattern of $Gd_{0.95}Eu_{0.05}BO_3$/AAO products, hydrothermally synthesized at 240 °C for 12 h.

3.2. Morphologies of $GdBO_3$:Eu^{3+} one-dimensional nanomaterials

The SEM images of $GdBO_3$:Eu^{3+}/AAO products are shown in Fig. 2. Fig. 2a is the SEM image of $GdBO_3$:Eu^{3+} nanorods deposited

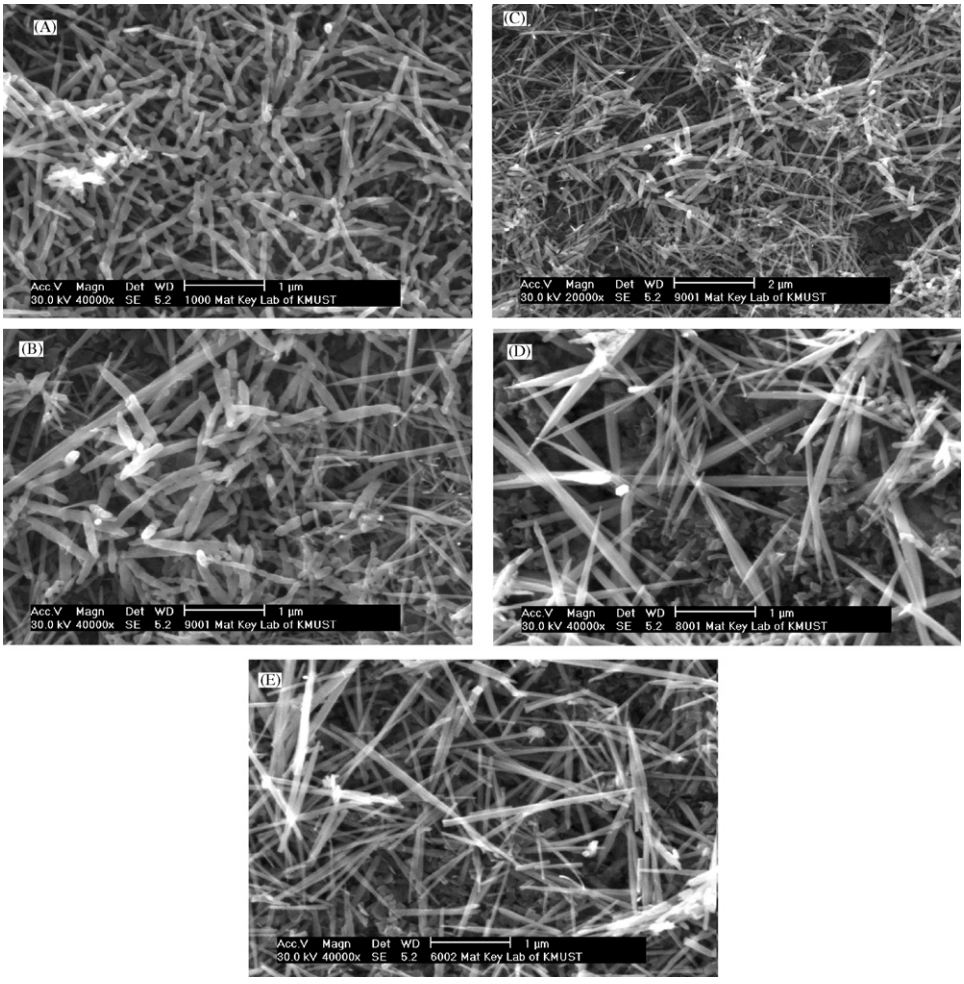

Fig. 2. SEM images of $Gd_{0.95}Eu_{0.05}BO_3$ deposited on the AAO template surface after calcined at different temperatures for 10 h. (a) 1000 °C; (b) 900 °C, high magnification; (c) 900 °C, low magnification; (d) 800 °C; (e) 600 °C.

on the AAO template surface after calcined at 1000 °C for 10 h. The diameters and length of $GdBO_3$:Eu^{3+} nanorods are 50–160 nm and 0.5–2 μm, respectively. Fig. 2b and c is the high magnification and low magnification SEM images of the as-prepared products deposited on the AAO template surface after calcined at 900 °C for 10 h, respectively. They show that the layer is composed of nanorods and nanoribbons. The length of most of nanorods and nanoribbons is 1–2 μm. The maximum length of a nanoribbon in Fig. 2c is ~10 μm. Fig. 2d and e is the SEM images of the as-prepared products deposited on the AAO template surface after calcined at 800 and 600 °C for 10 h, respectively. Only nanoribbons with length of 1–3 μm can be seen from Fig. 2d and e.

Since a hydrothermal process was employed to prepared the $GdBO_3$:Eu^{3+}/AAO samples, the $GdBO_3$:Eu^{3+} absorbed on the AAO template surface is very active, and calcined to form one-dimensional materials with different morphologies along a special direction on the AAO template surface at a certain calcination temperature. As it is well known, $GdBO_3$ possess low-temperature phase (LT phase) and high-temperature one (HT phase) [39]. Differential thermal analysis (DTA) of $GdBO_3$ shows that there is an endothermal peak at 912 °C in the curve of heating up, indicating there is a solid–solid phase transition at this temperature (912 °C), the phase transition between the LT and HT phase begins at 836 °C in the DTA curve of heating up[39]. Based on the structural phase transition of $GdBO_3$, we can explain the change of the morphologies of $GdBO_3$:Eu^{3+} one-dimensional materials at different calcination temperature. The LT phase is stable below 836 °C, calcined at 600 and 800 °C, the morphologies of the $GdBO_3$ nanomaterials are both nanoribbons. Between 836 and 912 °C, the LT and HT phases of $GdBO_3$ can exist together, so the morphologies of the $GdBO_3$ nanomaterials are composed of nanorods and nanoribbons after the $GdBO_3$:Eu^{3+} samples treated at 900 °C. Above 912 °C, the LT phase is transformed completely to the HT phase, so only nanorods exist in the $GdBO_3$:Eu^{3+} samples after calcined at 1000 °C.

When calcined at high temperature, the $GdBO_3$:Eu^{3+} samples are tightly attached to AAO template, and the $GdBO_3$ nanomaterials cannot be separated from $GdBO_3$:Eu^{3+}/AAO samples by ultrasonic method, so transmission electron microscopy (TEM) measurement was not done and the growth direction of the $GdBO_3$ nanomaterials was not determined. The growth mechanism of $GdBO_3$:Eu^{3+} one-dimensional materials with different morphology deposited on the AAO template surface is under the way.

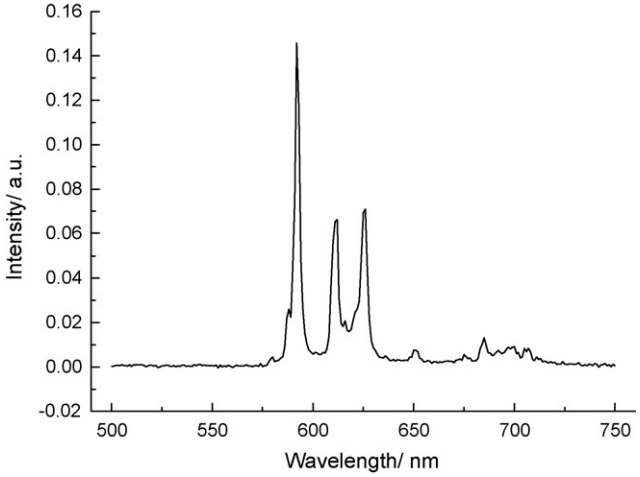

Fig. 3. Emission spectrum of $Gd_{0.95}Eu_{0.05}BO_3$/AAO products under 160 nm VUV excitation after calcined at 900 °C for 10 h.

3.3. Luminescent properties of $GdBO_3$:Eu^{3+}/AAO samples

Fig. 3 displays the emission spectrum of $GdBO_3$:Eu^{3+}/AAO products under 160 nm VUV excitation. The spectrum consists of lines ranging from 580 to 750 nm, which are assigned to the transitions from the excited $^5D_0$ level to ^7F_J (J = 1, 2, 3, 4) levels of Eu^{3+} activators. The major emissions of the as-prepared products are at 591 nm ($^5D_0 \rightarrow {}^7F_1$) and 610 and 625 nm ($^5D_0 \rightarrow {}^7F_2$), which are consistent with those of $GdBO_3$:Eu^{3+} powders prepared by the common solid state reaction [3–5]. The PL results also show that the one-dimensional nanomaterial deposited on the AAO template surface is $GdBO_3$:Eu^{3+}.

4. Conclusions

Eu^{3+} doped $GdBO_3$ nanorods and nanoribbons were morphology-controlled grown via a hydrothermal process combined with high-temperature calcination. The morphologies, crystal structures and luminescent properties of the nanomaterials were characterized. The morphologies of the nanomaterials were controlled by calcination temperature, and the changed morphologies of the nanomaterials at different temperatures were explained by the structural phase transition of $GdBO_3$. XRD and PL studies indicate that the one-dimensional materials deposited on the AAO template surface are hexagonal vaterite-type $GdBO_3$:Eu^{3+}.

Acknowledgement

This project was financially supported by the Natural Science Foundation of Yunnan Province (2007B201M).

References

[1] A.W. Veenis, A. Bril, Philips J. Res. 33 (1978) 124–132.
[2] Z. Yang, M. Ren, J.H. Lin, M.Z. Su, Y. Tao, W. Wang, Chem. J. Chin. Univ. 21 (2000) 1339–1343.
[3] Z.Y. Zhang, Y.H. Zhang, X.L. Li, J.H. Xu, Y. Huang, J. Alloys Compd. 455 (2008) 280–284.
[4] D. Boyer, G. Bertrand-Chadeyron, R. Mahiou, C. Caperaa, J.C. Cousseins, J. Mater. Chem. 9 (1999) 211–214.
[5] K.N. Kim, H.K. Jung, H.D. Park, J. Mater. Res. 17 (2002) 907–910.
[6] D. Boyer, G. Bertrand, R. Mahiou, J. Lumin. 104 (2003) 229–237.
[7] K.Y. Jung, E.J. Kim, Y.C. Kang, J. Electrochem. Soc. 151 (2004) H69–H73.
[8] L.S. Wang, J. Lin, Y.H. Zhou, Chem. J. Chin. Univ. 25 (2004) 11–15.
[9] M. Tukia, J. Holsa, M. Lastusaari, J. Niittykoski, Opt. Mater. 27 (2005) 1516–1522.
[10] Z.H. Li, J.H. Zeng, Y.D. Li, Small 3 (2007) 438–443.
[11] X.C. Jiang, L.D. Sun, C.H. Yan, J. Phys. Chem. B 108 (2004) 3387–3390.
[12] X.C. Jiang, C.H. Yan, L.D. Sun, Z.G. Wei, C.S. Liao, J. Solid State Chem. 175 (2003) 245–251.
[13] X.C. Jiang, L.D. Sun, W. Feng, C.H. Yan, Cryst. Growth Des. 4 (2004) 517–520.
[14] T. Kim, S. Kang, Mater. Res. Bull. 40 (2005) 1945–1954.
[15] F.S. Wen, W.L. Li, Z. Liu, T. Kim, K.Y. Yoo, S.H. Shin, J.H. Moon, J.H. Kim, Solid State Commun. 133 (2005) 417–420.
[16] J. Zhang, J. Lin, J. Cryst. Growth 271 (2004) 207–215.
[17] H.L. Zhu, L. Zhang, T.T. Zuo, X.Y. Gu, Z.K. Wang, L.M. Zhu, K.H. Yao, Appl. Surf. Sci. 254 (2008) 6362–6365.
[18] X. Guo, Y.H. Wang, J.C. Zhang, J. Cryst. Growth 311 (2009) 2409–2417.
[19] Y.F. Xu, D.K. Ma, X.A. Chen, D.P. Yang, S.M. Huang, Langmuir 25 (2009) 7103–7108.
[20] G.H. Pan, H.W. Song, X. Bai, Z.X. Liu, H.Q. Yu, W.H. Di, S.W. Li, L.B. Fan, X.G. Ren, S.Z. Lu, Chem. Mater. 18 (2006) 4526–4532.
[21] L.M. Chen, H. Cheng, G.C. Liu, X.C. Duan, J. Am. Ceram. Soc. 91 (2008) 591–594.
[22] G.H. Pan, H.W. Song, L.X. Yu, Z.X. Liu, X. Bai, Y.Q. Lei, L.B. Fan, S.Z. Lu, X.G. Ren, J. Nanosci. Nanotechnol. 7 (2007) 593–601.
[23] J. Yang, C.M. Zhang, L.L. Wang, Z.Y. Hou, S.S. Huang, H.Z. Lian, J. Lin, J. Solid State Chem. 181 (2008) 2672–2680.
[24] R.S. Yadav, R.K. Dutta, M. Kumar, A.C. Pandey, J. Lumin. 129 (2009) 1078–1082.
[25] H.W. Song, H.Q. Yu, G.H. Pan, X. Bai, B. Dong, X.T. Zhang, S.K. Hark, Chem. Mater. 20 (2008) 4762–4767.
[26] Z.G. Wei, L.D. Sun, C.S. Liao, C.H. Yan, Appl. Phys. Lett. 80 (2002) 1447–1449.
[27] A.E. Henkes, R.E. Schaak, J. Solid State Chem. 181 (2008) 3264–3268.
[28] R.F. Service, Science 294 (2001) 2442–2443.
[29] D. Appell, Nature 419 (2002) 553–555.
[30] Y.N. Xia, P.D. Yang, Y.G. Sun, Y.Y. Wu, B. Mayers, B. Gates, Y.D. Yin, F. Kim, H.Q. Yan, Adv. Mater. 15 (2003) 353–389.

[31] F. Zhou, X.M. Zhao, Y.Q. Liu, C.G. Yuan, L. Li, Eur. J. Inorg. Chem. 16 (2008) 2506–2509.
[32] H.L. Zhu, D.R. Yang, G.X. Yu, H. Zhang, D.L. Jin, K.H. Yao, J. Phys. Chem. B 110 (2006) 7631–7634.
[33] Q.Y. Lu, F. Gao, S. Komarneni, Chem. Mater. 18 (2006) 159–163.
[34] G.C. Xi, K. Xiong, Q.B. Zhao, R. Zhang, H.B. Zhang, Y.T. Qian, Cryst. Growth Des. 6 (2006) 577–582.
[35] H. Masuda, K. Fukuda, Science 268 (1995) 1466–1468.
[36] C. Zhang, F. Tao, G.Q. Liu, L.Z. Yao, W.L. Cai, Mater. Lett. 62 (2008) 246–248.
[37] X.H. Tan, J. Alloys Compd. 477 (2009) 648–651.
[38] Z. Yang, F. Song, X.L. Wang, Chem. J. Chin. Univ. 29 (2008) 1532–1534.
[39] M. Ren, J.H. Lin, Y. Dong, L.Q. Yang, M.Z. Su, L.P. You, Chem. Mater. 11 (1999) 1576–1580.